Geomorphology 131 (2011) 85–97

Contents lists available at ScienceDirect

Geomorphology

journal homepage: www.elsevier.com/locate/geomorph

Post-last glacial alluvial fan and talus slope associations (Northern Calcareous Alps, Austria): A proxy for Late Pleistocene to Holocene climate change

Diethard Sanders *, Marc Ostermann

Institute of Geology and Palaeontology, University of Innsbruck, Innrain 52, 6020 Innsbruck, Austria

ARTICLE INFO

Article history:
Received 11 October 2010
Received in revised form 14 April 2011
Accepted 24 April 2011
Available online 30 April 2011

Keywords:
Alps
Quaternary
Talus
Scree slope
Glacial–interglacial
Paraglacial

ABSTRACT

Near Innsbruck city (Austria, Eastern Alps), following the Last Glacial Maximum (LGM), an alluvial fan-to-talus slope succession was supplied from a carbonate-rock cliff more than 1000 m in height. $^{234}U/^{230}Th$ ages of 9.5 to 9.37 isotope kyrs of diagenetic cements in the alluvial-fan succession suggest that the fan/talus deposit accumulated mainly during late-glacial to, perhaps, early Holocene times. The deepest-exposed interval of the fan succession contains cracked lithoclasts probably fractured by overburden from late-glacial ice; this interval is topped by an intra-sequence unconformity. Following final glacial retreat, and rapid aggradation of the alluvial fan and talus slope, the geomorphic regime changed to erosion, as recorded by fanhead trenching and cutting of fluvial terraces, abandonment and vegetating of scree slopes, and excavation of 'talus flatirons'. The changeover from the accumulation of fan and talus to abandonment and dissection probably took place during the terminal late-glacial interval to perhaps the early Holocene. This erosional regime persists until present.

A record of rapid late-glacial to early Holocene accumulation of an alluvial fan/talus deposit followed by: (i) abandonment and vegetation growth, combined with (ii) cutting of intra-sequence unconformities of limited lateral extent, is typical of Alpine mountain-flank deposystems situated at comparatively low altitudes. This record consists of (a) an autocyclic component, that is, progressive lowering of sediment input due to onlap and burial of freshly-deglaciated mountain flanks supplying alluvial fans and talus slopes, and (b) an allocyclic component, that is, deglacial climatic warming and upward rise of an altitudinal range with a maximum number of freeze-thaw cycles ('talus window'), also leading to progressive vegetation-induced hillslope stabilization and lowering of scree production.

1. Introduction

In the Alps, proglacial successions deposited in valleys blocked by advancing ice streams are well-known (e. g., Fliri, 1973; Van Husen, 1977; de Graaff, 1996). Proglacial intramontane deposystems were characterized by high accumulation rates chiefly as a result of hillslope stripping and increase in physical weathering (Van Husen, 1983). Because the Alpine ice streams of the Last Glacial Maximum (LGM) probably decayed within a thousand years at most (Van Husen, 2004), deglaciation was associated with a pulse of rapid paraglacial to late-glacial sediment accumulation. The term paraglacial encompasses 'earth-surface processes, sediments, landforms, landsystems and landscapes that are directly conditioned by former glaciation and deglaciation' (Ballantyne, 2002; cf. Church and Ryder, 1972). Paraglacial relaxation of mountain flanks may include rockslides (Ballantyne, 2002; Prager et al., 2008), slow deep-seated gravitational mass wasting (Kellerer-Pirklbauer et al., 2010), and rapid shedding of coarse clastic material (Sanders et al., 2009). Deglaciation, however, was punctuated by standstills and by stadial re-advances of valley glaciers (Ivy-Ochs et al., 2009; Thompson Davis et al., 2009). In the Eastern Alps, the time span between decay of major, pleniglacial ice streams and the onset of the Holocene comprises the late-glacial interval, ranging from ~21.1 ka to 11.7 ka BP (Preusser, 2004; Ivy-Ochs et al., 2006, 2009). Most late-glacially active deposystems such as alluvial fans and talus slopes are situated at comparatively low altitudes, and today are abandoned and vegetated, and/or undergoing erosion. For valleys of the Northern Calcareous Alps (NCA), based on seismic surveys, Schrott et al. (2004) conclude that late-glacial to Holocene alluvial fans and talus slopes comprise the largest sediment storage in these areas. Relative to other intramontane deposits, scree slopes have been subject to few investigations with respect to their long-term development over thousands of years. This may, in part, result from the fact that talus deposits in most cases are devoid of soil layers that can be age-dated by the radiocarbon method.

Intramontane successions accumulated over glacial–interglacial cycles consist of unconformity-bounded units that represent landward correlatives, or partial correlatives, to marine glacio-eustatic sequences. Depending on sediment input (cf. Schlager, 2004), marine

* Corresponding author.
E-mail address: Diethard.G.Sanders@uibk.ac.at (D. Sanders).

0169-555X/$ – see front matter © 2011 Elsevier B.V. All rights reserved.
doi:10.1016/j.geomorph.2011.04.029

sequences are characterized by overall continuous deposition over glacial–interglacial and stadial–interstadial cycles; thus, intra-sequence unconformities most commonly are absent (Van Wagoner et al., 1988; Mitchum and Van Wagoner, 1991). Conversely, in intramontane successions, because of drastic fluctuations of sediment input from deglaciation to 'stable' interglacial conditions, switches from sedimentation to erosion and associated cutting of intra-sequence unconformities are common. In this paper, an example of accumulation of a 'low-altitude' alluvial fan-to-talus slope deposit is described in detail in an area that, today, is largely abandoned and undergoing erosion (area A in Fig. 1). Post-glacial talus slopes that today are abandoned and dissected into 'talus flatirons' are common in the NCA (e. g., area B in Fig. 1; see discussion below). The sedimentary record suggests a paraglacial start of talus accumulation that continued, after a potential late-glacial advance of locally-sourced ice, during the late-glacial to early Holocene interval; this is supported by $^{234}U/^{230}Th$ disequilibrium ages of interstitial calcite cement. A subsequent changeover from aggradation to dissection resulted in cutting of laterally-limited intra-sequence unconformities. Intra-sequence unconformities are common in intramontane successions, and form due to the turnover from paraglacial/late-glacial sediment accumulation to an interglacial erosive regime.

2. Methods

The described succession was investigated in repeated field trips over an interval of ten years; this reduced bias from seasonally-changing outcrop conditions that are typical for unlithified sedimentary successions. Isohypsed satellite orthophotographs and laserscan images (both down to 1:2000), provided free by the federal government of the Tyrol (http://tiris.tyrol.at), improved precision in mapping, altitude leveling of outcrops, and identification of geomorphic elements. Cut rock slabs and thin sections served for documentation of lithification and features of diagenesis. For $^{234}U/^{230}Th$ disequilibrium dating of diagenesis, layers of skalenohedral calcite that formed along interstitial vadose water tables were age-dated (see Ostermann et al., 2006, 2007; Sanders et al., 2010, for detailed description of method).

3. Geological setting

The NCA consist of a stack of cover thrust nappes dominated by Triassic platform carbonates (Neubauer et al., 1999; Schmid et al., 2004). Alpine orogenic deformation was multi-phase and heteroaxial (Eisbacher and Brandner, 1996), resulting in densely-spaced faulting and jointing, especially of carbonate rocks. Subsequent to Neogene uplift (Schmid et al., 2004), during the Quaternary, the Alps were subject to at least four major glaciations (Van Husen, 2004). Erosion by Quaternary glaciations still drives slow uplift of the Central Alps (Norton et al., 2010). The present scenery of the western NCA was almost entirely shaped by Quaternary glaciations: deeply-incised, U-shaped valleys are bounded by rock cliffs that locally rise directly to summits, or that are associated with glacial cirques, hanging valleys and glacial shoulders.

In the western sector of the NCA, with respect to thickness and geomorphic significance, two stratigraphic units stand out, (a) the

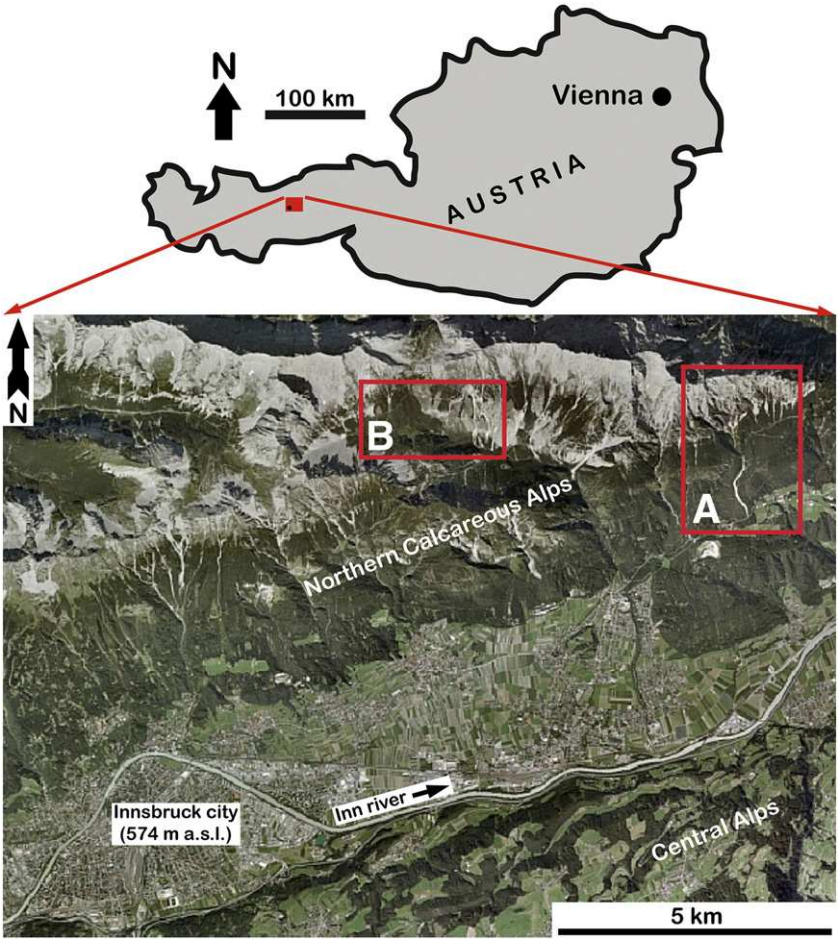

Fig. 1. Geographic position of Innsbruck in Austria and of areas mentioned in the text. A: Urschenbach; B: Iss valley.

Wetterstein Limestone (Middle to early Late Triassic), and (b) the Hauptdolomit unit (Late Triassic pro parte) (Table 1). In the study area, a belt of tectonic slivers composed of stratigraphic units of Early Triassic to Early Cretaceous age is also present (Fig. 2; Table 1); the slivers formed in a wrench belt sub-parallel to the major Inn-valley strike-slip fault (Delago, 2005). The Inn-valley glacier of the LGM is recorded by three types of index clasts: (a) dark-green colored garnet amphibolites derived from a source near the origin of the Inn river; (b) granites with greenish feldspars, also derived from near the origin of the Inn, and (c) light green to whitish, diablastic garnet amphibolites rich in feldspar derived from the Oetz valley in the Oetztal-Stubai basement unit, along the middle reach of the Inn.

Up-section, in the area of Gnadenwald-Urschenbach (Fig. 2), the exposed Quaternary succession consists of several units (Table 2): (1) banded lacustrine silts and clays deposited in a periglacial climate, (2) a package of gravelly fluvial deposits accumulated from glacial outwash ahead of the advancing Inn glacier, and (3) a veneer of basal till of the Inn glacier of the LGM. Together, units (1) to (3) make-up a comparatively wide and long terrace (Gnadenwald terrace; Fig. 2). The basal till (unit 3, Table 2) is overlain and downlapped by unit (4a), an 'old' alluvial fan that accumulated during late-glacial to earliest Holocene time (Fig. 2, Table 2). Subsequent to accumulation, the old alluvial fan became incised by the Urschenbach creek, giving rise to unit (4b), a system composed of the stream channel, terraces, and a 'young' alluvial fan perched in a lower position onto the old fan (Fig. 2; see also Fig. 5). Today, the young alluvial fan is covered by pine forest. Urschenbach is a semi-perennial creek fed by a spring emerging below the high cliffs of Walderkamp Spitz (Fig. 2). The downslope lateral extent of the water-run part of the creek, however, varies by a factor of about 2.5 with the seasons. Upslope of and contiguous with the alluvial fan (unit 4a), a large talus slope covered by forest comprises unit 5a (Fig. 2, Table 2). This talus is partly lithified, and abandoned. In the proximal part of slope, the talus is shaped by erosionally-incised, wide chutes into 'flairons'; the flatirons are forested by *Pinus mugo* (see also Fig. 7). The incised chutes, in turn, are paved by active scree slopes which represent unit 5b (Table 2). The active scree slopes, however, all terminate between about 1450–1600 m a.s.l.

4. Sedimentary facies and facies associations

Prevalent sedimentary facies are characterized in Table 3, wherein references to Figs. 3 and 4 are also indicated. Herein, facies associations are distinguished only for successions exposed in outcrops sub-vertical to bedding; deposystems exposed with their surface, such as active scree slopes, are not included. Two facies associations are distinguished:

(1) Alluvial fan association characterized by rudites of cohesive debris flows, intercalated with water-laid rudites (cf. Table 3). In the Urschenbach alluvial fan, from the *stratigraphically* deepest outcrops (located at about 1110 m a.s.l.) to the stratigraphically topmost exposed layers (930–920 m a.s.l.), clasts of the Ruhpolding Radiolarite, Adnet-Klauskalk Formation, Hauptdolomit unit, Northern Alpine Raibl beds and clasts of metamorphic rocks, including index clasts of the LGM, are present. In total, however, the fan succession is strongly dominated by clasts of Wetterstein Limestone. With fluctuations, lithoclasts of units other than Wetterstein Limestone become extremely rare towards the stratigraphically highest exposed levels of the fan at 920–930 m a.s.l. In addition, in the fan succession, clasts of talus breccias were found in strata of cobbly openwork breccias (Fig. 4C and D). These clasts, in turn, consist of clast-supported breccias, with a clast spectrum that can be derived from the local rock substrate, similar to the succession hosting the talus-breccia clasts. One clast of talus

Table 1
Stratigraphic units in the investigated area. For interpretations of lithologies, the reader is referred to cited references. Formal rank and ranges of units are taken from the Stratigraphic Chart of Austria (Piller et al., 2004). Stratigraphic units in bold are of outstanding significance in building mountains and cliffs. The other units all are present in tectonic slivers in a belt corresponding to 'The Slope' (see Fig. 2).

Stratigraphic unit; total stratigraphic range	Characteristic lithologies in the investigated area	Remarks, References
Alpiner Buntsandstein to Werfen beds; Lower Triassic (Induan to Olenekian)	Fluvial to marginal-marine clastics: Red to pink sandstones, siltstones and claystones	Stingl (1989)
Reifling Formation; Lower to Middle Triassic (Bithynian to Cordevolian)	Deep-water limestones: Wavy-bedded, spiculithic wackestones to packstones	Brandner (1984)
Partnach beds; Middle Triassic (Langobardian to Cordevolian)	Succession of basinal environment: Black claystones to marly black lime mudstones	Brandner (1984)
Wetterstein Limestone; up to about 1000 m thick Middle to Upper Triassic	Limestones of shallow-water platform: Light gray, very thick-bedded, e. g., lime mudstones, cryptmicrobially-laminated limestones, loferites	Builds the south-facing cliffs ('Upper Cliffs') of Walderkampspitz (Fig. 2). Brandner (1984)
(Illyrian to Cordevolian) Northern Alpine Raibl beds; Upper Triassic	Variegated rocks of neritic environments, typically (a) onco-rud/floatstones; (b) black lime mudstones; (c) cellular dolomites, (d) micaceous sandstones to siltstones	Bechstädt and Schweizer (1991)
(Julian and Tuvalian) *Hauptdolomit unit;* up to about 1500–2000 m thick Lower and Middle Norian (Lacian and Alaunian)	Dolostones of shallow-water platform: Monotonous, ocre- to brown-gray weathering dolostones, typically sucrosic at surface	Substrate of 'bedrock gorge'; builds the 'Lower Cliffs' (Fig. 2) Brandner (1984)
Adnet Formation; Hettangian to Aalenian Klauskalk Formation; Bajocian to Oxfordian	Red, condensed, nodular deep-water limestones with ammonites	Lithoclasts of Adnet and Klauskalk Formation, respectively, may be hardly distinguishable Gawlick et al. (2009)
Ruhpolding Radiolarite; Oxfordian	(a) Red to green to blackish radiolarian chert, (b) red cherty marlstones with radiolaria	
Ammergau Formation; Kimmeridgian to Valanginian	Deep-water limestones with radiolaria, benthic foraminifera, and few planktic foraminifera	
Schrambach Formation; Valanginian to Aptian	Light-red to pink, marly, stylonodular deep-water limestones to marls; with ammonite aptychi	

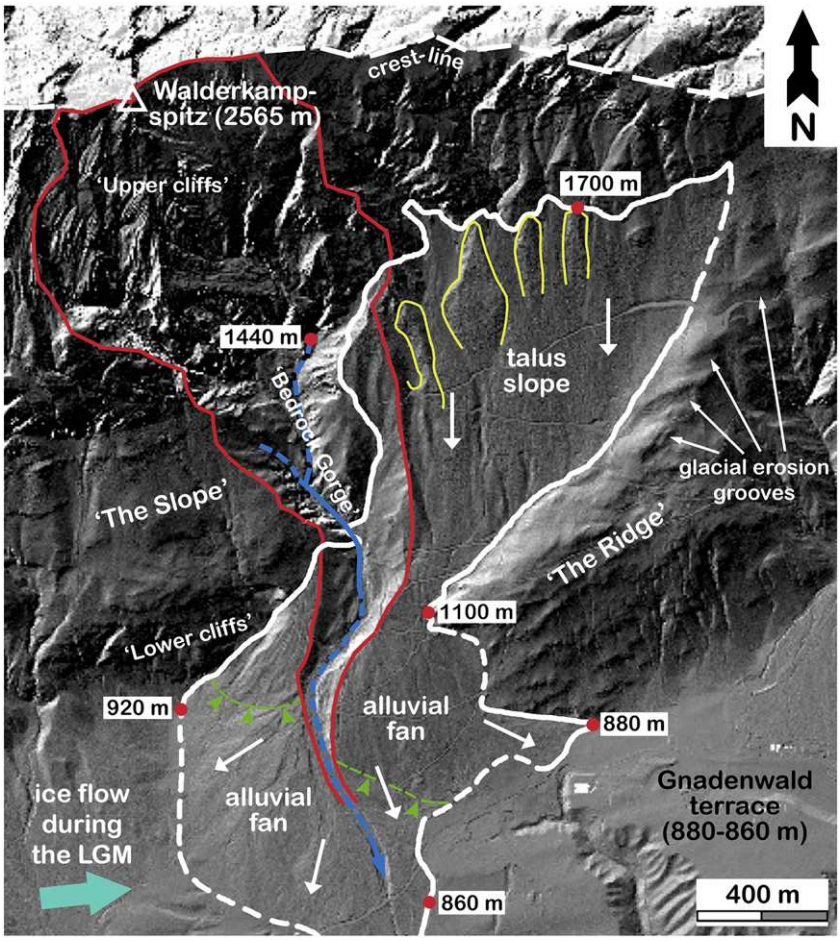

Fig. 2. Laserscan overview of Urschenbach alluvial fans and talus slope. Following the Last Glacial Maximum (LGM), an alluvial fan ('old alluvial fan' in figure; unit 4a in Table 2) downlapped and prograded over a wide terrace (Gnadenwald terrace; see also Table 2); up-section, the terrace consists of proglacial lake deposits, overlain by glacial outwash and basal till of the Inn-valley glacier of the LGM. Subsequent to its maximum aggradation, the old alluvial fan became subject to erosional incision. Incision of the old fan gave rise to a younger stream channel-alluvial fan system ('young alluvial fan' in figure; unit 4b in Table 2) perched in lower position; incision persists until present. Approximate limit between the old and young alluvial fan, respectively, is indicated by dashed green line with arrowtips. Red line: topographic drainage area of the present channel-fan system. Dashed blue line indicates ephemeral watershed; continuous blue line shows approximate extent of perennial watershed. Main morphological features (cliffs, ridges, slopes) are indicated by tagged 'names'. The talus slope (unit 5a in Table 2) shows a distal onlap onto 'The Ridge', a rock ridge veneered by glacial till of the LGM, and with grooves and whalebacks produced by glacial erosion. In its proximal part, the talus slope is shaped by incision of chutes into flatirons (hightlighted by yellow outline, see Fig. 7 for details). The incised chutes, in turn, are paved by active scree slopes (unit 5b in Table 2). The light-blue arrow indicates the overall direction of ice flow of the Inn-valley glacier during the Last Glacial Maximum.

breccia, found in a cobbly openwork fabric, was coated by a flowstone cement that also coated other, adjacent clasts in the same clast fabric (Fig. 4D). Within the Urschenbach fan succession, including and above the stratigraphically lowest outcrop C (Fig. 5), the clast spectrum is strongly dominated by clasts of Wetterstein Limestone derived from the Upper Cliffs. In addition, a small number of clasts derived from The Slope (clasts of Hauptdolomit unit and younger units up to the Ruhpolding Formation) is consistently present. At the exit of the small bedrock gorge incised into The Slope, an interval about 1 m thick of alluvial conglobreccia rich in cobbles to boulders of Ruhpolding Formation is present. The richness of this conglobreccia in clasts of Ruhpolding Formation, and in particular in cobbles to boulders, is much greater than that of all the other outcrops of the Urschenbach fan. The conglobreccia unconformably overlies a package of alluvial breccias of different character (steeper dip, much better sorting, richer in clasts of Wetterstein Limestone, with infiltrated lime mud matrices). In addition, similar alluvial breccias rich in clasts of Ruhpolding Formation were found in outcrops at 870–890 m in a low terrace along the presently active channel.

(2) Talus-slope association. This association (see Table 3) is exposed mainly in anthropogenic exposures up to a few meters in vertical extent, along the road to Hinterhorn Alm (Fig. 2). At and close to 1400 m a.s.l., the roadcut provides exposures of the lithified talus. The talus slopes consist of strata dipping about 30° to the south. The strata consist of poorly to extremely poorly sorted, small-bouldery to gravelly breccias with a matrix of carbonate-lithic wackestone to packstone; in addition, the matrix locally contains mica flakes as well as sand- to fine-gravel sized metamorphic rock fragments. The association is dominated by clast-supported breccias with a primary matrix of lime mud. Lenses and laterally-elongated lenses of openwork fabrics are rare. The talus slopes exposed in roadcuts are abandoned and densely vegetated by *P. mugo*. In addition, at least in their proximal to apical part, the abandoned talus slopes are lithified. Conversely, the presently active scree slopes occur in chutes incised into the vegetated, abandoned and lithified talus slopes; the chutes paved by the active scree slopes erode the lithified talus into 'flatirons'. Despite careful search, no index clasts of the Inn-valley glacier of the LGM, and no gravel-sized clast of metamorphic rock were found within

Table 2
Quaternary depositional units in the investigated area, from oldest (number 1) to youngest (numbers 4b, 5b). LGM = Last Glacial Maximum. Compare with Fig. 2.

Unit number / Unit name / Characteristics and interpretation		References, remarks
'Gnadenwald terrace	#1 'Bändertone' (banded silts and clays): Banded silts and clays with fossils indicative of a cold (periglacial or distal-proglacial) lacustrine environment. Age: Late Würmian, before LGM. Radiocarbon ages of organic remnants in middle part of section: 36,300 ± 1700 and 31,900 ± 1500 yr cal ^{14}C BP	Fliri (1973), Klasen et al. (2007)
	#2 'Vorstoß-Schotter' (glacial outwash ahead of advancing Inn glacier): Fluvial gravels rich in clasts of metamorphic rocks from the Central Alps, including index clasts of Inn-valley glacier of LGM (see text). Gravels accumulated from sandar ahead of the advancing Inn glacier. Age: Late Würmian, closely before LGM	Fliri (1973), Patzelt and Resch (1986)
	#3 'Grundmoräne des Inngletschers' (basal till of Inn glacier): Basal till with index clasts of Inn-valley glacier of LGM (see text). LGM: 24–21.5 kyr cal BP	Patzelt and Resch (1986); see Preusser (2004) and Ivy-Ochs et al. (2004), for range of LGM
#4a Old alluvial fan: Alluvial fan above the basal till of Inn glacier (unit #3), and containing index clasts of the LGM. Phase of fan aggradation: Late-glacial to earliest Holocene. Alluvial fan became incised by younger Urschenbach channel-terrace-alluvial fan system (unit 4b)		This paper
#4b Younger channel-terrace-alluvial fan system: Ephemerally-active stream channel and terraces, incised progressively deeper with time into old alluvial fan. Trenching and incision of the old alluvial fan (unit 4a) perhaps started during the early Holocene, and led to development of a younger alluvial fan (now abandoned) perched in lower position on the old alluvial fan		This paper
#5a Vegetated talus: Partly lithified, abandoned talus, vegetated over its entire extent. Shaped by erosion into 'talus flatirons' in the proximal part of slope. Phase of talus accumulation: mainly late-glacial; waning talus activity during Holocene		This paper
#5b Scree slopes: Slopes composed of loose scree consisting exclusively of clasts of Wetterstein Limestone derived from southern cliff of Walderkampspitz. Scree slopes are present in incised, wide chutes between flatirons of older talus (unit 5a)		This paper

or on top of the abandoned, lithified talus flatirons. In thin section, however, the matrix of lithified talus breccias may contain sand-sized metamorphic rock fragments. The stratification of the lithified talus-slope breccias is visible, either by slight changes in back- and out-weathering of strata, and/or by intercalated lenses of openwork clast fabrics, and dips with about 30° to south, sub-parallel with the presently active talus slopes. In all cases, the strike/dip of stratification of the lithified breccias fits the present morphology and general strike of the rock cliff above.

4.1. Cracked lithoclasts

In the stratigraphically deepest levels in the northern part of outcrop A (Fig. 5), as well as in outcrops B and C, in lenses and strata with openwork clast fabrics, lithoclasts cracked at sub-vertical point contacts are common. Clasts involved in cracking range up to cobble size (Fig. 4D–F). The cracking may be confined to single, smaller clasts under- and overlain by larger clasts; in many of these cases, cracking obviously propagated from point contacts among clasts. Some clasts may be broken into angular pieces by shear. The resulting rock fragments are sharp-edged, thin, splinter-like chips. In other cases, fractures propagate vertically over two to three lithoclasts of up to cobble size. In one case, a gravel-sized clast of garnet-bearing mica schist was found to be cracked in directions subnormal to schistosity (Fig. 4E). The cracked clasts were found only in the stratigraphically deep levels of the fan succession (Fig. 5A). In the higher levels and in their lateral, more distal equivalents, no cracked clasts were observed. Similarly, in the partly lithified talus successions, no cracked clasts were identified.

4.2. Diagenesis and U/Th age of cement

4.2.1. Alluvial-fan succession

In the alluvial fan succession, features of lithification and cementation are common and varied (Table 4). In the Urschenbach fan, an overall trend to increasing lithification with increasing stratigraphic depth is obvious. Where the former fan surface can be considered as largely preserved, lithification starts a few meters below the surface, but is typically confined to openwork layers. In stratigraphically deeper levels, lithification tends to become more pervasive, and affects openwork layers (diverse types of cements) and layers with primary and secondary matrices of lime mud (lithification of mud, dissolution pores fringes by cement). In outcrop C, in openwork clast fabrics of conglobreccias, isopachous cement fringes of scalenohedral calcite precipitated at vadose interstitial water tables were observed; these were sampled for U/Th dating (red star labeled 1 in Fig. 5A). The calculated ages suggest cement precipitation between about 9.5 to 9.37 ka (Fig. 6). The potential significance of these ages is discussed below. In both outcrop A and B, in gravelly to cobbly layers with openwork fabric, a few lithoclasts bear soda-straw stalactites, and/or are coated by flowstone crusts up to about 2 mm in thickness (see also Sanders et al., 2009).

4.2.2. Scree slopes

In field and thin section, well-developed fringes of cement are thin and scarce in the lithified talus. The talus successions are mainly affected by lithification of the lime-muddy matrix, via dissolution and reprecipitation on a sub-microscopic scale (Table 4). In the talus breccias with a primary matrix of lime mud, in cut slabs and thin section, macro- to megapores are common; these pores may show a relatively 'even' outline, or they may abut the adjacent matrix along

Table 3
Prevalent facies of investigated succession. For easier communication of sediment characteristics, the name of their lithified counterpart is used (e. g., 'conglobreccia' instead of: ruditic deposit composed of subequal amounts of rounded and angular clasts'). Clasts of Triassic carbonate mentioned herein are derived from the local rock substrate. LGM = Last Glacial Maximum.

Facies group	Facies	Interpretation, figure reference, literature references
Water-laid rudites	Sheet-flow deposits: Gently lense-shaped packages (20–50 cm thick) of (a) a lower part of well-sorted, coarse to medium gravels arranged subparallel to bedding, or in downstream-imbricated fabrics; and (b) an upper part of fine gravel to coarse sand with subparallel lamination Strata dip with 25° to a few degrees Gravelly openwork fabrics may contain a secondary matrix of geopetally-laminated lime mudstone	Deposits of shallow sheet-like water flows accumulated during waning flood stage Fig. 3A and B (Sanders et al., 2009)
	Channel-fills: Lenticular units (strike section) or with wavy lower boundary (dip section) of subrounded to very well-rounded cobbles to small boulders; clasts include Triassic carbonate rocks from local substrate, and clasts of metamorphic rocks including also the index lithologies of the LGM; dip section: downstream-imbricated gravels to small boulder common	Conglobreccias to conglomerates deposited during waning flood stage within stream channels Fig. 3C (Sanders et al., 2009)
Debris-flow rudites	Cohesive debris-flows: Clast-supported, moderately to extremely poorly sorted, gravelly to small-bouldery deposits with a matrix of carbonate-lithic 'wackestone to packstone'; no vertical clast segregation, disordered clast fabric vertically across intervals; lithoclastic fraction may be represented by angular to rounded clasts of Triassic carbonate rocks mixed with rounded metamorphic rock fragments (including index clasts of LGM), or of clasts of Triassic rocks only	Breccias to conglobreccias deposited from cohesive debris flows Figs. 3C–F, 4A and B (Sanders et al., 2009)
	Grain-flow deposits: Dipping (25–35°) lenses to sheets of clast-supported, well-sorted to poorly sorted, gravelly to cobbly openwork rudites	Breccias deposited from cohesionless, gravelly to cobbly debris flows (Sanders et al., 2009)
Lenses of openwork clast fabric	Lenses of openwork clast fabrics: Lenses a few clasts up to about 50 cm in thickness of openwork gravels to cobbles, intercalated in cohesive debris-flow breccias	Facies difficult to assign to a single origin. Openwork clast fabrics may form by processes (that may act in combination), such as: (a) deposition of veneers and small depositional lobes of openwork clast fabrics from ephemeral surface runoff on cohesive debris-flow deposits, by clast transport in surface runoff, and/or by eluviation of matrix from cohesive debris-flow deposits, and/or (b) frost-coated clast flows (the latter a category of debris flow) Figs. 3C, 4B–F (Sanders et al., 2009; Sanders, 2010)

an extremely irregular, pitted boundary. In the lime-muddy matrix of the talus breccias, small fenestral/vesicular pores may result from several processes, such as entrapment of air during sediment transport, segregation of water during freezing, and vadose dissolution. The highly irregular, pitted outline of some fenestral pores suggests that at least these resulted from dissolution, or from dissolution overprinting of pores of other origin. In clast fabrics that originally contained a matrix of lime mud, vesicular megapores up to a few centimeters in width are present. The pores may be coated by a thin isopachous fringe of scalenohedral calcite cement, or may be unfringed. The matrix of lime mud, by contrast, is firm but friable.

5. Morphostratigraphic relations

5.1. Alluvial fan

Laserscan satellite images, combined with the observation that the Urschenbach fan contains scattered LGM index clasts, indicate that the fan downlaps onto the underlying sheet of basal till of the LGM Inn-glacier on top of the Gnadenwald terrace (cf. Fig. 2). Overall, the deeply incised trench within the present alluvial fan indicates that it underwent erosion over a long interval of time. Progressive erosional downcutting is recorded by terraces preserved at different levels along Urschenbach (Fig. 5) and, in the lower part of the fan, by flanks of abandoned channels incised in progressively lower positions into the fan (Fig. 5A). At 1040 m a.s.l. along Urschenbach, in outcrop C, there is an unconformable contact between: (a) an underlying package of moderately steeply southward-dipping breccias that are partly lithified, and that consist of openwork clast layers and layers of breccia with a primary matrix of lime mud; and (b) a sharply overlying interval composed of unlithified, winnowed carbonate-lithic sand with rounded gravels to small boulders (Fig. 3). The latter interval corresponds to a terrace (Fig. 5A). In the upper part of outcrop D (Fig. 5B), strata dip at 25–30° to the south (dip was estimated by visual bearing with a clinometer from opposite valley flank). At its right bank, the bedrock gorge incised into the cliffs of Hauptdolomit terminates sharply at the vertical wall of the Lower Cliffs (Fig. 5B). Both the alluvial breccias rich in clasts of Wetterstein Limestone and the overlying cobbly to bouldery conglobreccia rich in clasts of Ruhpolding Formation can be traced in outcrop for a few meters into the bedrock gorge, where they onlap the right-hand bedrock flank.

5.2. Talus slopes

The post-glacial talus slopes that onlap the toe of the 'Upper cliffs' (southern cliff of Walderkampspitz, Fig. 2) consist of two parts. (i) abandoned, lithified talus; this talus is shaped by erosional incision into 'talus flatirons' densely vegetated by *P. mugo* (Fig. 7). (ii) chutes a few tens to about 100 m in width that are veneered by the presently-active, unvegetated scree slopes (Fig. 7). Both the lithified talus flatirons and the active scree chutes are cut in a criss-cross pattern by the road to Hinterhorn Alm. Downslope, the surface of the talus flatirons and of the scree chutes merge. Despite detailed search along the road cut into the talus slopes, no metamorphic rock fragments of gravel size were found; this suggests that the lithified talus was not veneered by glacial drift of the LGM, i.e. it is probably of post-glacial age.

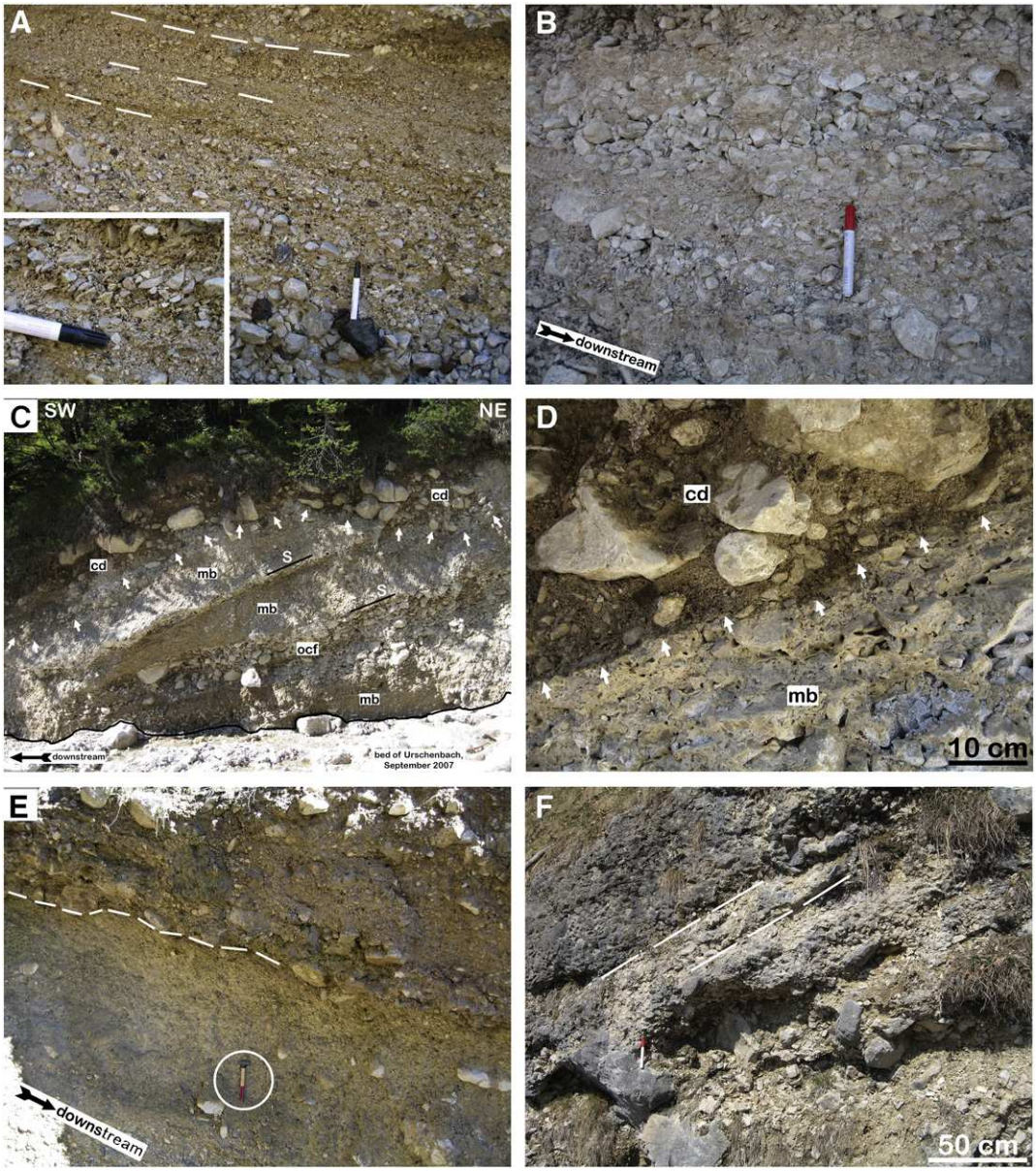

Fig. 3. Sedimentary facies: (A) Stratified breccia composed of clasts of carbonate rocks and, subordinately, of dark red to blackish clasts of radiolarian cherts. Pen is 14 cm long. Inset: Angular to subangular lithoclasts arranged in downstream-imbricated fabric. Pen is 15 mm in diameter; (B) Outcrop of alluvial fan succession at left bank of Urschenbach, 930 m a.s.l. The package in photo consists of: (a) strata of moderately-sorted gravels with openwork fabric, vertically interbedded with (b) strata of poorly- to moderately-sorted, gravelly sand to sand. Pen is 14 cm long; (C) Outcrop C, 1040 m a.s.l., September 2007. A package of partly lithified breccias, dipping with 20–30° south (stratification labeled S) consists of: (a) poorly sorted breccias (mb) with a primary matrix of lime mud; these are intercalated with (b) lenses of gravelly to cobbly openwork clast fabrics (ocf). Within the latter, clasts fractured at interstitial point contacts are common (Fig. 4E and F). The breccia package is truncated (truncation labeled by white arrows) and overlain by unlithified, gravelly to small-bouldery stream-channel deposits (cd) of subangular to well-rounded clasts. Width of view 8 m; (D) Detail of truncation surface of Fig. 3C: Poorly sorted breccia (mb) with a primary matrix of lime mud riddled by vesicular megapores. The breccia is sharply overlain, along a surface of erosion (labeled by arrows) by gravelly to small-bouldery stream-channel deposits (cd) with a matrix of winnowed, unlithified sand; (E) Layer of outweathering, extremely poorly sorted breccia rich in cobbles to small boulders of radiolarian chert derived from the Ruhpolding Formation (cf. Table 1). The breccia sharply overlies better-sorted, overall finer-grained breccias that, in turn, are rich in clasts of carbonate rocks and poor in clasts of radiolarian chert. Encircled hammer is 35 cm in length; (F) Outcrop at 1400 m a.s.l. of talus breccia. The package consists of steeply (~30 °C) south-dipping strata of gravelly to small-bouldery deposits. The clasts consist of Wetterstein Limestone derived from the cliffs ('Upper Cliffs') of Walderkampspitz summit higher upslope (see Fig. 2).

6. Interpretation

6.1. Alluvial fan and talus slope

Because the Urschenbach fan contains LGM index clasts scattered throughout the exposed succession, and because the fan downlaps the basal till of the LGM Inn glacier, we infer that fan and talus deposition started after deglacial ice decay (starting at ~21.1 isotope kyrs BP; Ivy-Ochs et al., 2006). Furthermore, we assume that upon reforestation of the Inn valley (~17.4 cal kyrs BP to ~15 cal kyrs BP; Patzelt, 1980, 1987; Van Husen, 2004) and associated hillslope stabilization, the accumulation rates on fan and talus slopes diminished. As further outlined below, U/Th ages of 9.5 to 9.37 isotope ka of cements in the alluvial-fan succession support the hypothesis that the main phase of fan aggradation was terminated by the early Holocene.

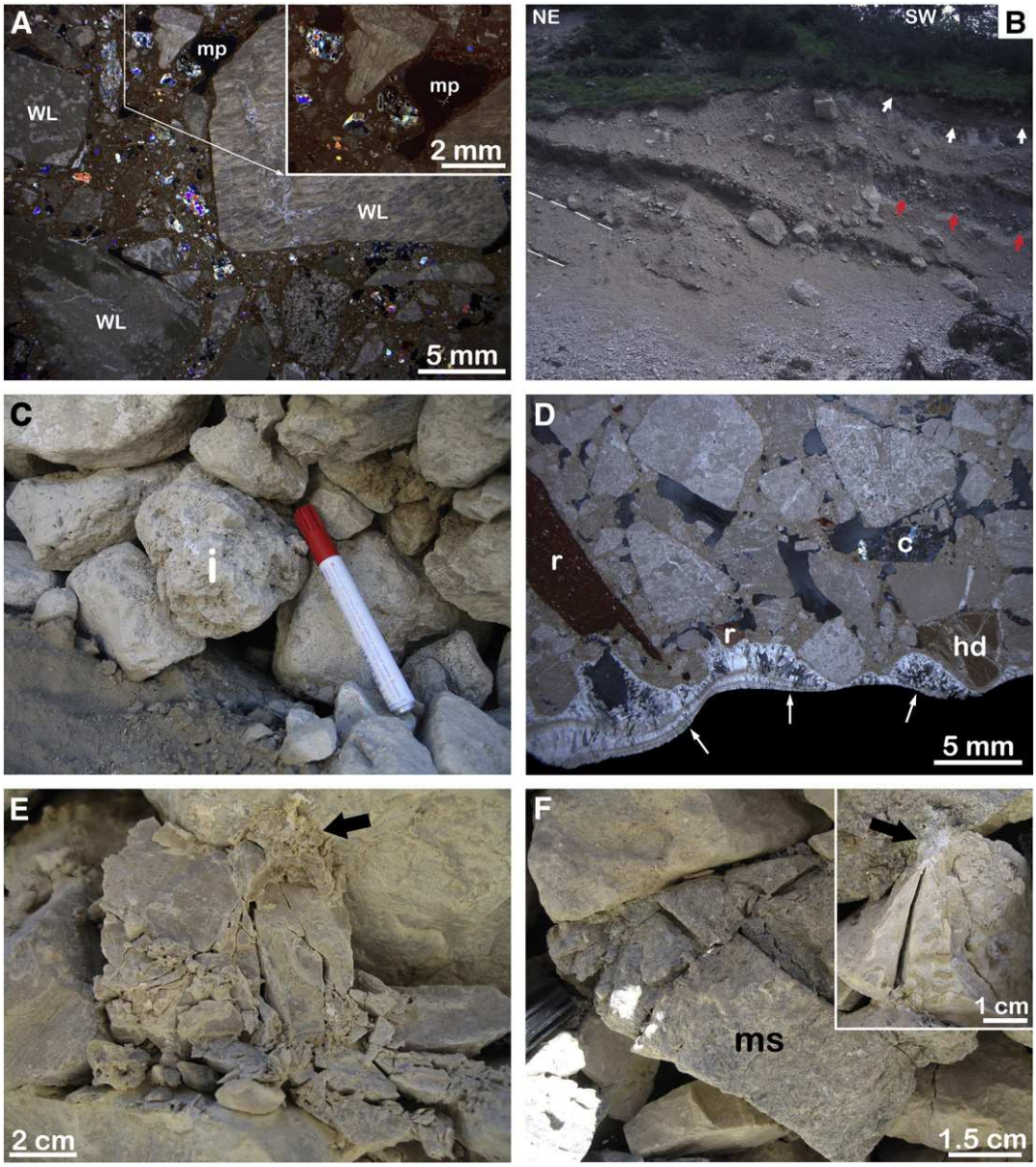

Fig. 4. Sedimentary facies: (A) Thin section of talus breccia shown in Fig. 3F. The clast spectrum is dominated by clasts of Wetterstein Limestone (a few labeled WL). In addition, clasts of quartzites and mica schists are present. The matrix, a lithic packstone, is riddled by megapores (black patches, mp) of irregular outline. Crossed nicols. Inset: Aside of megapore (mp), note clasts of Wetterstein Limestone (WL) and clasts of quartzites (colored patches). Crossed nicols; (B) Northern part of outcrop B (September 2007). Package of strata, dipping with about 20–30° south. The package consists of: (a) breccias with a primary matrix of lime mud, and with angular boulders of carbonate rocks, and (b) outweathering, gentle lenses of angular, coarse gravelly to cobbly openwork clast fabrics; in these latter deposits, fractured clasts (see text) are present up to at least the level labeled by the red arrows. In addition, the openwork clast fabrics are partly lithified by very thin crusts of micritic cement, and locally contain crusts of post-depositional flowstone and stoda-straw stalactites. This package is sharply overlain, along a surface labeled by white arrows, by unlithified, darker-colored sands and gravels. Width of view approximately 20 m; (C) Coarse-gravelly to cobbly openwork clast fabric composed mainly of clasts of Wetterstein Limestone, with intraclast (i) of a talus breccia. Urschenbach, 975 m a.s.l., outcrop A (cf. Fig. 5A); (D) Thin section of intraclast of talus breccia. The intraclast, in turn, consists of a clast-supported breccia with a macro- to megaporous matrix of lithic wackestone. Aside of the majority of clasts derived from the Wetterstein Limestone (gray clasts), a few clasts from the Hauptdolomit unit (hd) as well as radiolarites (r) and cherts (c) from the Ruhpolding Formation are present. The intraclast of talus breccias is coated by a fringe of flowstone (indicated by white arrows). Crossed nicols; (E) Clast of Wetterstein Limestone crunched along numerous fractures; the main fractures propagate from the point contact (labeled by black arrow) to the overlying clast. Urschenbach, 1040 m a.s.l., outcrop C (cf. Fig. 5B); (F) Clast of mica schist (ms, coated by micritic dust), fractured along two main fracture sets perpendicular to schistosity (plane visible in photo). The other clasts in the photo consist of Wetterstein Limestone. Inset in upper right: After careful removal of the clast of mica schist in front, underneath, a clast of Wetterstein Limestone appeared that was fractured at point contacts. Arrowtip points to whitish cataclastic powder typical of impact or loading.

As mentioned previously, up to at least 1400 m a.s.l. the matrix of post-glacial, lithified talus slopes contains mica flakes and small metamorphic rock fragments; whereas mica flakes may stem from aeolian input, the sand-sized metamorphic rock fragments most probably are derived from glacial drift. Today, save small patches vegetated by *P. mugo*, the 'Upper Cliffs' expose only bare Wetterstein Limestone (cf. Fig. 2). The presence of small metamorphic rock fragments in the post-LGM talus breccias thus may suggest that a large, or perhaps the major, volume of talus accumulated rapidly after deglaciation at site.

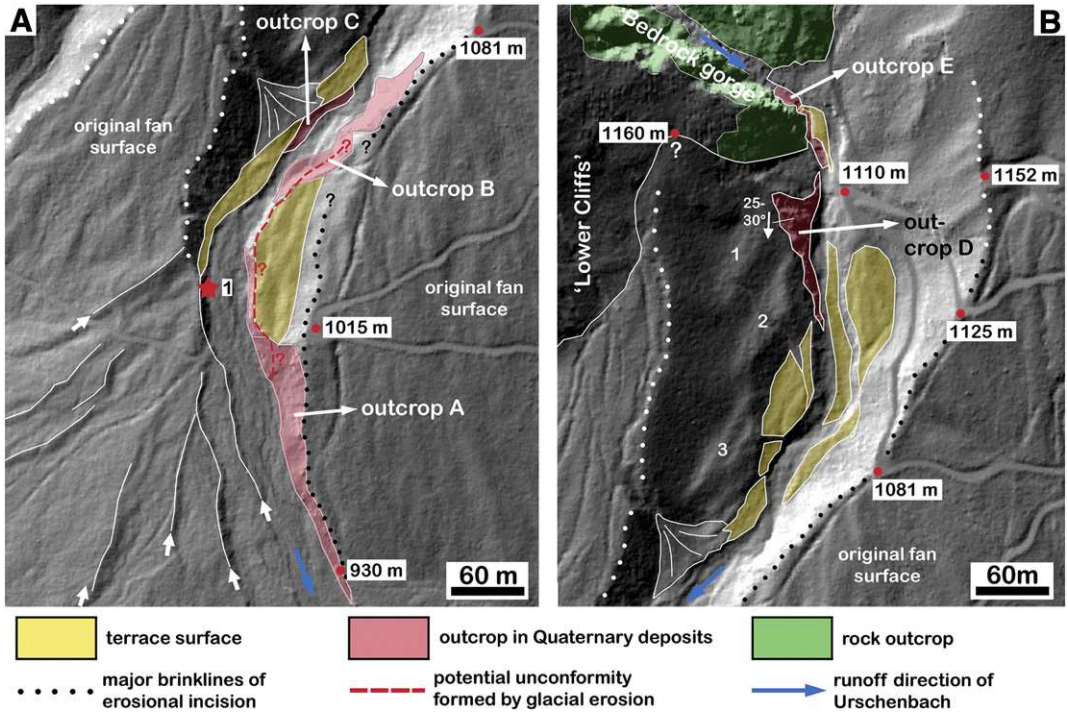

Fig. 5. Laserscans of Urschenbach fan: (A) Lower part of fan (see also Fig. 2). The proxy 'original fan surface' (fan surface at time of maximum local aggradation) today is covered by pine forest. The fan succession is exposed in three outcrops labeled A to C. Dashed red line with question tags marks the approximated position of an unconformity (see text). Upon erosional incision of the fan, channels were cut down to progressively deeper levels (white lines mark right-hand channel flanks, some labeled by small white arrows). The red stars labeled 1 to 3 mark the locations of samples taken for U/Th age-dating of diagenetic cement (see text); (B) Upper part of fan: Subsequent to its maximum aggradation up to at least 1160 m a.s.l., the fan became erosionally incised. Indistinct surfaces labeled 1 to 3 may represent high-positioned, old terraces formed during early fan incision. Younger terraces (yellow) are clearly identifiable. In the stratigraphically higher part of outcrop D, strata dip with 25–30° to south. In outcrop E, lithified alluvial breccias extend upstream into and onlap the right flank of the 'Bedrock Gorge'.

6.2. Morphostratigraphy

Morphostratigraphic relations indicate that the alluvial fan/talus-slope deposits were formed by an initial phase of net aggradation followed by cutting of intra-sequence unconformities. Intra-sequential unconformity development is recorded by incision of partly lithified talus flatirons, and by progressive trenching of the alluvial fan and excavation of terraces; both, talus dissection and fanhead trenching may have started at a similar time. In the upper part of outcrop C, the strata dipping with 25–30° to south indicate that, at or close to its maximum aggradation, the *proximal to apical* part of the alluvial fan had the characteristics of a steep-dipping talus cone. The preservation of alluvial breccias in the bedrock gorge, in onlap onto the gorge flank, indicates that at least the lower reach of the gorge already existed before accumulation of the present Urschenbach fan. Because of erosion, the former maximum extent of onlap of the alluvial fan is difficult to estimate. Taking the highest preserved fan deposits at 1160 m a.s.l., however, and projecting their dip upslope suggests that the fan might have aggraded to roughly 1250 m a.s.l.: In this stage, the proximal part of the Urschenbach fan had the shape and steepness of a talus cone. Even in this stage, however, the outcrop of Ruhpolding Formation was partly exposed, providing clasts of radiolarite and chert.

6.3. Diagenesis

Because of the sampling method for U/Th dating by chipping off a piece of water-table cement and using it in bulk for dating, the calculated ages (without 2 σ standard error) may average a period of a few hundred years. Notwithstanding such potential imprecision, cement precipitation between about 9.5 to 9.37 ka indicates that the alluvial fan was already in place by that time. In talus breccias with a primary matrix of lime mud, primary fenestral pores may form by air entrapment during sediment transport, for instance, in a cohesive debris flow or in a solifluction sheet. Alternatively, intrinsic fenestral porosity may form from ice segregation (cf. Van Vliet-Lanoe, 1976; Bertran and Texier, 1999). Secondary fenestral pores can form by selective dissolution of diagenetically unstable lithoclasts (Sanders,

Table 4
Features of diagenesis. See Sanders et al. (2010) for interpreation of diagenetic products.

Feature	Interpretation, remarks
Semi-lithified (friable) lime-muddy matrix, with vesicular macro- to megapores locally fringed by isopachous calcite cement	Semi-lithified lime mud: Produced by dissolution-reprecipitation of $CaCO_3$ on submicroscopic scale Vesicular pores fringed by isopachous cement: Change from vadose conditions to an essentially phreatic environment
Micritic cements on lithoclasts: menisci, fringes and/or mammillary crusts	Precipitation of micritic $CaCO_3$ in vadose diagenetic environment
Water-table cements	Precipitation of micrite to calcite orthospar along water tables (vadose environment) in megapores of openwork clast fabrics
Flowstone crusts and soda-straw stalactites on/below lithoclasts in openwork fabrics	Speleothems of vadose diagenetic environments

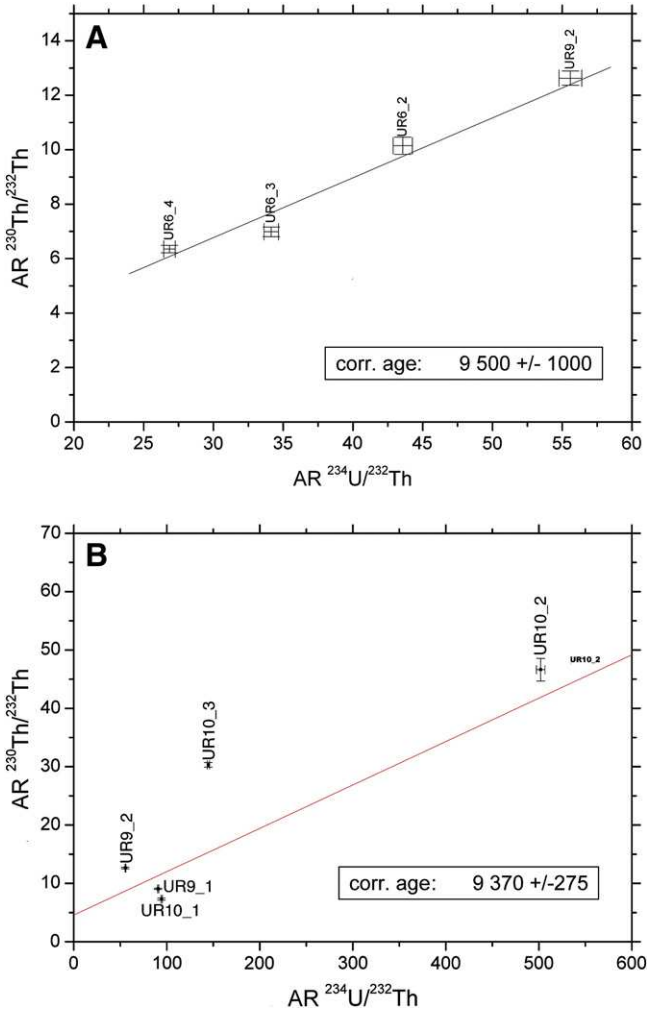

Fig. 6. Plots of $^{234}U/^{232}Th$ activity ratio (AR) versus $^{230}Th/^{232}Th$ activity ratio ('Rosholt diagram') of samples of diagenetic cements in the alluvial-fan succession (see Fig. 5A for location). In both diagrams, the slope of the regression line between sub-sample plots is used to calculate corrected activity ratios for age calculation (see text). The 'corrected' calculated age for each sub-sample set is indicated in a box in lower right in each sub-figure A and B.

2010). Vesicular pores, in turn, may be difficult to distinguish in polished slab and thin section from fenestrae; vesicular pores demonstrably form in the vadose zone along networks of percolating groundwater, by eluviation/dissolution of the matrix (Sanders et al., 2010). For the intra-sequence unconformity (Fig. 3C and D), the observation that vesicular pores are widest and most common just beneath the contact with the overlying, unlithified sediments of the 're-incision phase' of Urschenbach suggests that these pores developed by intense hyporheic groundwater flow. The observation that these pores are fringed by calcite cement indicates that, in a late stage of their development, they were percolated by pore waters supersaturated with respect to calcite.

The talus flatirons below Walderkampspitz are part of a larger array of similar flatirons in this area. Towards the west, along south-facing cliffs of Wetterstein Limestone, flatirons of partly lithified talus slopes of post-glacial age are present (Delago, 2005; Ostermann, 2006). Meteoric lithification, or partial lithification confined to specific layers, of talus slopes thus can take place within a few hundreds to thousands of years after accumulation. Limited or partial lithification, such as cement precipitation within specific layers, is common in post-glacial talus slopes composed of limestone clasts (Sanders et al., 2010).

6.4. Intraclasts

If the described intraclasts of talus breccias had been transported in frozen state, they should have fallen apart upon melting while enclosed in the layers of openwork clast fabric they were identified within (see Fig. 4C and D). To prevent disintegration of frozen intraclasts, one may postulate continuous permafrost; but then, alluvial-fan deposition is precluded. Lithification of intraclasts cannot be explained by 'separate' lithification of lime mud in a vadose-meteoric environment while intraclasts remained intact; in this case, the intraclasts were crushed by mechanical compaction well before any significant lithification of the lime muddy-matrix. In addition, we did not find evidence for lithified talus relicts older than the LGM. The conclusion thus seems inescapable that lithified talus deposits were eroded during accumulation of the Urschenbach fan.

In a well-preserved, lithified alluvial-fan to talus-slope succession north of Innsbruck ('Hötting Breccia' *Auct.*; at least most of it of earliest Würmian age), different types of intraclasts had been interpreted as products of erosion along intra-sequence unconformities (Sanders, 2008). That talus successions may sufficiently lithify for intraclast production within a few hundreds to a few thousands of years after deposition, and in relatively shallow levels, is underscored by the erosionally-incised talus slopes in the investigated area described herein, and by lithified post-glacial talus flatirons in Hall valley (area B in Fig. 1). Intermittent erosion of early-lithified talus may be one reason why talus intraclasts are comparatively common in Quaternary mountain-flank successions of the NCA (Sanders, 2008, 2010; Sanders et al., 2010).

6.5. Significance of cracked lithoclasts

The interval with cracked lithoclasts (Fig. 4E and F) is difficult to interpret. With ground acceleration caused by seismic waves, lithoclasts embedded under sufficient overburden can be cracked. Along the Inn valley, historical earthquakes (16th and 17th century) have attained an estimated magnitude of 4.5 to 5.2 Mercalli-Sieberg. Clast cracking upon propagation of earthquake waves, however, tends to be arranged along discrete, sub-vertical planes; this is not the case for the observed cracked clasts. Alternatively, the clasts were cracked by overburden from glacial ice. After the LGM, perhaps within a few hundreds of years, the ice streams decayed to about 50% of their maximum extent (Van Husen, 2004); after that first glacial retreat, the area of Urschenbach was probably ice-free, but located near the left margin of the 'Bühl-stadial' Inn glacier (Van Husen, 2004; cf. Ivy-Ochs et al., 2006). Re-investigation of Bühl-stadial type locations led Reitner (2007) to abandon that stadial, and to introduce the concept of 'early late-Glacial ice decay' (ELGID); accordingly, the ELGID-Inn glacier consisted largely of stagnant ice prone to down-wasting. At the same time, the advance of glaciers with smaller catchments in the NCA was triggered by debuttressing (Reitner, 2007). After the ELGID halt of the Inn glacier, the Inn valley was not reached by stadial ice advances (cf. Ivy-Ochs et al., 2006); the Inn valley was permanently ice free at ~17.4 kyr cal BP over most of its extent (Van Husen, 2000, 2004). Together, this implies that the interval with the cracked lithoclasts may have formed between the onset of ice decay at about 21.1isotope kyr BP and ice-free conditions in the Inn valley at ~17.4 kyr cal BP. Clast cracking by late-Glacial ice loading requires a retreat of ice beyond the deposit with the cracked clasts, to allow for paraglacial accumulation of that part of the talus, followed by ice re-advance. This was achieved either by (a) hypothetical fluctuations of the lateral margin of the ELGID Inn glacier, or (b) by glacial debuttressing and consequent advance of locally-supplied ice; the latter hypothesis is supported by the observation that advance of local glaciers proceeds only after a lag time of decay of the main ice stream, and over deposits recording a separation in space between the downwasted ice stream and laterally-advancing local ice (cf. Reitner,

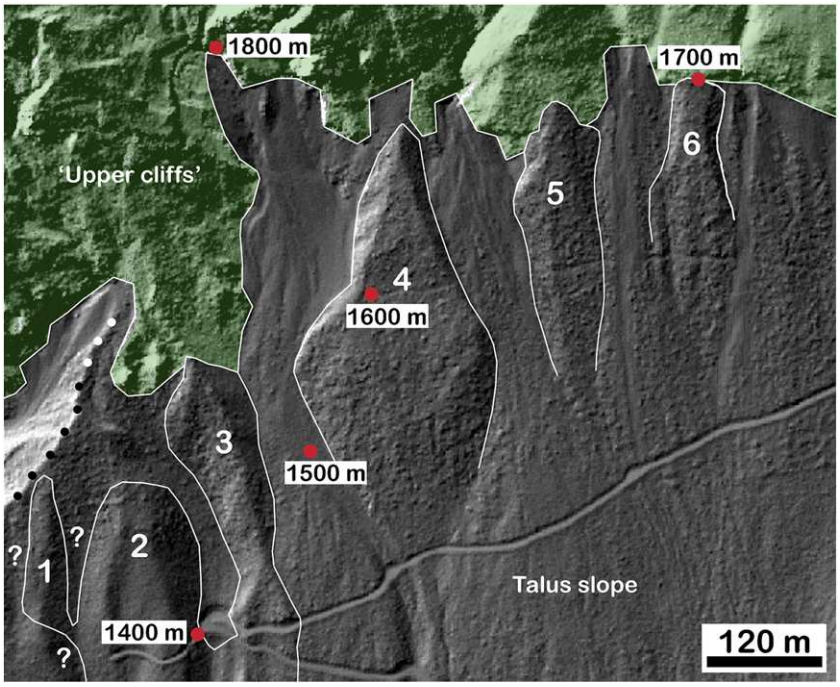

Fig. 7. Laserscan of talus slope below the rock cliffs ('Upper Cliffs') of Walderkampspitz (see Fig. 2). Within the slope, talus 'flatirons' numbered 1 to 6 are visible. The flatirons are densely vegetated by *Pinus mugo*, and weather out because they are lithified. The unlithified active scree slopes fill wide chutes incised between the talus flatirons.

2007). Alternatively, in openwork clast fabrics, overburden by a few tens of meters of sediment may suffice to induce fracture at point contacts; it seems doubtful, however, whether the potential sediment load at location C (cf. Fig. 5) were sufficient.

Finally, the interval with the cracked clasts may be of pre-LGM age. Data to support this hypothesis, however, are absent. In any case, the well-preserved surface and shape of the Urschenbach fan/talus succession, as well as the absence of metamorphic rock fragments of gravel size or larger at the present fan- and talus surface shows that the surface was not overprinted by glacial erosion. This observation, combined with: (a) the absence of clast cracking in higher/more distal stratigraphic levels of the fan, and (b) the presence of cracked lithoclasts in a succession dominated by cohesive debris-flow deposits in the stratigraphically lowest-exposed part, suggest that these two sedimentary packages are separated by an intra-sequence unconformity. Apart from the clear-cut exposure in outcrop C, the intra-sequence unconformity surface could not be located with certainty in other outcrops.

7. Discussion

Accumulation of scree slopes proceeds most rapidly in an altitudinal range with a maximum frequency of freeze-thaw cycles ('talus window', Hales and Roering, 2005). In most natural situations, frost-induced weathering is driven by growth of segregation ice (Hallet et al., 1991; Matsuoka, 2001; Hall and André, 2003); this process probably is most effective between −3° to −6 °C (Murton et al., 2006). To understand the relationships between scree-slope development and altitude over thousands of years and more, however, the concept of the talus window nevertheless is an accepted proxy. Temperature records from Alpine cliffs suggest that the present talus window is located between about 2300 and 2800 m a.s.l. (cf. Gruber et al., 2004). The altitude of the talus window changes most strongly over glacial–interglacial and stadial–interstadial cycles, respectively (Hales and Roering, 2005). In the Alps, stadial lowerings of the equilibrium line altitude (ELA) of glaciers were in the range of hundreds of meters (Ivy-Ochs et al., 2006) and, by inference, the associated lowerings of the talus window and of the tree line were similar. The Holocene fluctuations of climate, and associated risings/lowerings of ELAs and treelines, were much smaller than those of stadial-interstadial cycles (Patzelt, 1980; Nicolussi and Patzelt, 2001; Nicolussi et al., 2005; Ivy-Ochs et al., 2009). With the potential exception of the deepest interval with cracked clasts (see above), however, the Urschenbach fan/talus deposit records only a single 'lateglacial-to-interglacial' cycle of aggradation to dissection. To date, stadial/interstadial changes, as well as Holocene millenial to decadal climatic changes (e. g., Nicolussi and Patzelt, 2000; Wurth et al., 2004; Joerin et al., 2006), could not be unequivocally identified in talus successions.

In the Alps, present rates of rock-cliff retreat of 0.01 to 0.2 mm/a are an order of magnitude lower than average rates of late-glacial cliff retreat (see summary in Matsuoka, 2008); this disparity may, in part, result from intermediate storage of scree within cliffs (Krautblatter and Dikau, 2007) and the lack of rare, large-scale rockfalls in records of modern rates (Matsuoka, 2008). On the other hand deeply dissected, abandoned low-altitude fans and talus slopes are widespread. For the Alps, numerous observations indicate that shedding of coarse-grained detritus supplying low-altitude fans and talus slopes was most rapid during the late-glacial (Van Husen, 1983; Sanders et al., 2009). Similar records of rapid, late-glacial talus accumulation followed by abandonment and dissection during the Holocene are observed, for instance, in Britain and New Zealand (Hinchliffe, 1999; Ballantyne, 2002; Curry and Morris, 2004; Hales and Roering, 2005). Recall that the cliff of Walderkampspitz still towers for up to more than 1000 m (Fig. 2). The slope succession, accumulated since deglaciation, thus should also contain rare larger rockfall events; nevertheless, the geomorphic regime had changed from accumulation to dissection (see Fig. 7). Over all, these observations emphasize that the rate of sediment delivery was higher during the late-glacial, as also supported by the U/Th ages of 9.5 to 9.37 isotope kyrs of cements in the alluvial-fan succession. From the southern cliff of Walderkampspitz towards the west, flatirons of abandoned and vegetated scree slopes, some of them partly lithified, are locally present (area B in Fig. 1). These talus flatirons similarly are of late-glacial to early Holocene age, as indicated by: (a) their position along the bedrock

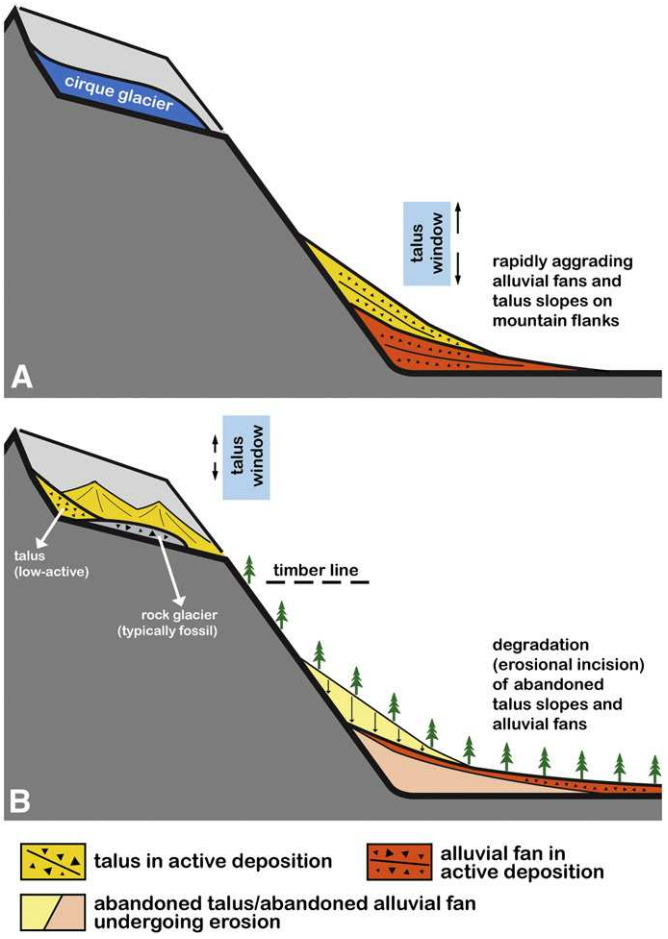

Fig. 8. Simplified scheme for post-glacial to present development of low-altitude alluvial fan-talus slope ensemble. (A) Upon deglaciation high, bare-rocky valley flanks became exposed to erosion; in addition, during late-glacial time, the 'talus window' (see text) fluctuated in comparatively low altitudes. This gave rise to rapid accumulation of alluvial fans and talus slopes along valley flanks. (B) Upon deglacial to Holocene climatic warming, the timber line shifted upwards, slopes became stabilized, and the previously active alluvial fans and talus were abandoned and subject to erosional degradation. Concomitantly, the talus window shifted to its present high altitude, where it supplies smaller talus slopes shed from comparatively lower cliffs that typically are situated around glacial cirques. See text for discussion.

flank of a glacially-shaped valley, and (b) absence of basal till on top, but the presence of LGM index clasts on the valley floors onto which the scree was shed. Unfortunately, in these talus flatirons, no cements suitable for age-dating were found (Ostermann, 2006). Nevertheless, these slopes also record a first phase of aggradation followed by abandonment, vegetation, and incision of scree-veneered chutes.

We suggest that the main reasons for rapid late-glacial sediment supply were: (a) the low position of the talus window (Fig. 8), combined with (b) enhanced physical weathering of glacially-weakened mountain flanks (cf. Ballantyne, 2002), and (c) immediately after decay of the Inn-valley ice stream, an initial vertical relief of the exposed, bare mountain flank roughly twice its present value (cf. Fig. 2). A large part of the Urschenbach fan/talus ensemble thus probably accumulated between the ELGID and reforestation in the Inn valley (~15 ka BP, see above) (Fig. 8). For the Central Alps, an upper treeline ecoline some 100–200 m higher in altitude than the year 2000-line is documented for ~9.6 to ~4.5 cal ka BP (Nicolussi and Patzelt, 2000, 2001; Tinner and Theurillat, 2003); on the average, summer temperatures during that interval may have been at least 1.0 °C higher than during 1920–1980 (Nicolussi et al., 2005). For the low-altitude Urschenbach fan/talus ensemble, this further supports the idea that vegetation-induced hillslope stabilization, excavation of talus flatirons, and significant fanhead trenching started during the early Holocene.

Aside from the potential intra-sequence unconformity, perhaps produced by late-glacial advance of locally-sourced ice, the changeover from: (a) net aggradation, to (b) abandonment and dissection produced intra-sequence unconformities of laterally limited extent. In the upslope portion of the deposystem, i.e. in the talus slopes, this is recorded by incision of scree-veneered chutes between partly lithified talus flatirons. On the alluvial fan, the re-incision of Urschenbach produced an intra-sequence unconformity characterized by: (a) fluvially-incised, steep to subvertical hillslopes, and (b) terraces cut down to successively lower levels. In mountain ranges subject to glacial–interglacial cycles, along valley flanks, intra–sequence unconformities are most probably widespread.

Late-glacial to Holocene warming led to an upward shift of the talus window to settings that strongly differ from late-glacial settings of scree accumulation. In the NCA and in carbonate-rocky terrains of the Central Alps, today, active talus is mainly situated in deglaciated cirques (Fig. 8). The activity of these scree slopes is low: For six selected areas, detailed comparison of high-resolution aerial photographs (1946–1954) with satellite orthophotographs (1999–2009) records only minor changes; these include: (a) widening and lengthening, or initiation, of channels passed by debris flows and ephemeral fluid flows, (b) downslope progradation, or new development of, alluvial fans, and (c) upward climb and/or densening of vegetation; there is no evidence for a significant increase in scree delivery from cliffs (Konrad, 2010). These observations fit with results from an other carbonate-lithic talus in the NCA (Heckmann et al., 2008). Thus, most the active carbonate-lithic scree slopes of the Eastern Alps today are in a state of low activity and/or incipient abandonment and dissection. Accumulation of alluvial fan/talus-slope ensembles in mountain ranges subject to glacial–interglacial cycles is non-steady in space and time, and is controlled by: (a) deglacial exposure of high, bare mountain flanks weakened by preceeding ice loading, ('paraglacial/periglacial influence'), (b) net upward shift of the talus window and of vegetation ('climatic influence'), and (c) a negative feedback between talus accumulation and rock-cliff degradation ('depositional influence'). In more general terms, the accumulation of fans and talus slopes is subject to both autocyclic and allocyclic controls.

Acknowledgements

Hanns Kerschner, Institute of Geography, Dieter Schäfer, Institute of Geology, and Gernot Patzelt, former Institute of High-Alpine Research, all at University of Innsbruck, are thanked for discussions as well as hints on literature. Financial support from project 16114-N06 of the Austrian Research Foundation is gratefully acknowledged.

References

Ballantyne, C.K., 2002. A general model of paraglacial landscape response. The Holocene 12, 371–376.
Bechstädt, T., Schweizer, T., 1991. The carbonate-clastic cycles of the East-Alpine Raibl group: result of third-order sea-level fluctuations in the Carnian. Sedimentary Geology 70, 241–270.
Bertran, P., Texier, J.-P., 1999. Facies and microfacies of slope deposits. Catena 35, 99–121.
Brandner, R., 1984. Meeresspiegelschwankungen und Tektonik in der Trias der NW-Tethys. Jahrbuch der Geologischen Bundesanstalt 126, 435–475.
Church, M., Ryder, J.M., 1972. Paraglacial sedimentation: a consideration of fluvial processes conditioned by glaciation. Geological Society of America Bulletin 83, 3059–3071.
Curry, A.M., Morris, C.J., 2004. Lateglacial and Holocene talus slope development and rockwall retreat on Mynydd Du, UK. Geomorphology 58, 85–106.
de Graaff, L.W.S., 1996. The fluvial factor in the evolution of alpine valleys and ice-marginal topography in Vorarlberg (W-austria) during the upper Pleistocene and Holocene. Zeitschrift für Geomorphologie, Neue Folge (Supplement 104), 129–159.
Delago, L., 2005. Geologie des Streifens Törl-Hinterhornalm (Nördliche Kalkalpen, Tirol). Unpubl. Diploma thesis, University of Innsbruck, 148 pp., 1 enclosure, 1 map.

Eisbacher, G.H., Brandner, R., 1996. Superposed fold-thrust structures and high-angle faults, Northwestern Calcareous Alps, Austria. Eclogae Geologicae Helvetiae 89, 553–572.
Fliri, F., 1973. Beiträge zur Geschichte der alpinen Würmvereisung: Forschungen am Bänderton von Baumkirchen (Inntal, Nordtirol). Zeitschrift für Geomorphologie, Neue Folge, Supplement 16, 1–14.
Gawlick, H.-J., Missoni, S., Schlagintweit, F., Suzuki, H., Frisch, W., Krystyn, L., Blau, J., Lein, R., 2009. Jurassic tectonostratigraphy of the Austroalpine domain. Journal of Alpine Geology 50, 1–152.
Gruber, S., Hoelzle, M., Haeberli, W., 2004. Rock-wall temperatures in the Alps: modelling their topographic distribution and regional differences. Permafrost and Periglacial Processes 15, 299–307.
Hales, T.C., Roering, J.J., 2005. Climate-controlled variations in scree production, Southern Alps, New Zealand. Geology 33, 701–704.
Hall, K., André, M.-F., 2003. Rock thermal data at the grain scale: applicability to granular disintegration in cold environments. Earth Surface Processes and Landforms 28, 823–836.
Hallet, B., Walder, J.S., Stubbs, C.W., 1991. Weathering by segregation ice growth in microcracks at sustained sub-zero temperatures: verification from an experimental study using acoustic emissions. Permafrost and Periglacial Processes 2, 283–300.
Heckmann, T., Haas, F., Wichmann, V., Morche, D., 2008. Sediment bugdet and morphodynamics of an alpine talus cone on different time scales. Zeitschrift für Geomorphologie, Neue Folge 52 (Supplement 1), 103–121.
Hinchliffe, S., 1999. Timing and significance of talus slope reworking, Trotternish, Skye, northwest Scotland. The Holocene 9, 483–494.
Ivy-Ochs, S., Schäfer, J., Kubik, P.W., Synal, H.-A., Schlüchter, C., 2004. Timing of deglaciation on the northern alpine foreland (Switzerland). Eclogae Geologicae Helvetiae 97, 47–55.
Ivy-Ochs, S., Kerschner, H., Kubik, P.W., Schlüchter, C., 2006. Glacier response in the European Alps to Heinrich event I cooling: the Gschnitz stadial. Journal of Quaternary Science 21, 115–130.
Ivy-Ochs, S., Kerschner, H., Maisch, M., Christl, M., Kubik, P.W., Schlüchter, C., 2009. Latest Pleistocene and Holocene glacier variations in the European Alps. Quaternary Science Reviews 28, 2137–2149.
Joerin, U.E., Stocker, T.F., Schlüchter, C., 2006. Multicentury glacier fluctuations in the Swiss Alps during the Holocene. The Holocene 16, 697–704.
Kellerer-Pirklbauer, A., Proske, H., Strasser, V., 2010. Paraglacial slope adujustment since the end of the Last Glacial Maximum and its long-lasting effect on secondary mass-wasting processes: Hauser Kaibling, Austria. Geomorphology 120, 65–76.
Klasen, N., Fiebig, M., Preusser, F., Reitner, J.M., Radtke, U., 2007. Luminescence dating of proglacial sediments from the Eastern Alps. Quaternary International 164–165, 21–32.
Konrad, F., 2010. Änderungen auf karbonat-lithoklastischen Schutthalden Tirols über einen Zeitraum von 50 bis 60 Jahren. Unpubl. B. Sc. thesis, Univ. of Innsbruck, 43 pp., with appendices.
Krautblatter, M., Dikau, R., 2007. Towards a uniform concept for the comparison and extrapolation of rockwall retreat and rockfall supply. Geografiska Annaler 89A, 21–40.
Matsuoka, N., 2001. Direct observation of frost wedging in Alpine bedrock. Earth Surface Processes and Landforms 26, 601–614.
Matsuoka, N., 2008. Frost weathering and rockwall erosion in the southeastern Swiss Alps: long-term (1994–2006) observations. Geomorphology 99, 353–368.
Mitchum, R.M., Van Wagoner Jr., J.C., 1991. High-frequency sequences and their stacking patterns: sequence-stratigraphic evidence of high-frequency eustatic cycles. Sedimentary Geology 70, 131–160.
Murton, J.B., Peterson, R., Ozouf, J.-C., 2006. Bedrock fracture by ice segregation in cold regions. Science 314, 1127–1129.
Neubauer, F., Genser, J., Handler, R., 1999. The Eastern Alps: result of a two-stage collision process. Mitteilungen der Österreichischen Geologischen Gesellschaft 92, 117–134.
Nicolussi, K., Patzelt, G., 2000. Discovery of early-Holocene wood and peat on the foreland of the Pasterze Glacier, Eastern Alps, Austria. The Holocene 10, 191–199.
Nicolussi, K., Patzelt, G., 2001. Untersuchungen zur holozänen Gletscherentwicklung von Pasterze und Gepatschferner (Ostalpen). Zeitschrift für Gletscherkunde und Glazialgeologie 36, 1–87.
Nicolussi, K., Kaufmann, M., Patzelt, G., van der Plicht, J., Thurner, A., 2005. Holocene tree-line variability in the Kauner valley, central Eastern Alps, indicated by dendrochronological analysis of living trees and subfossil logs. Vegetation History and Archaeobotany 14, 221–234.
Norton, K.P., Abbühl, L.M., Schlunegger, F., 2010. Glacial conditioning as an erosional driving force in the Central Alps. Geology 38, 655–658.
Ostermann, M., 2006. Thorium-uranium age-dating of "impure" carbonate cements of selected Quaternary depositional systems of western Austria: results, implications, problems. Unpubl. Ph. D. thesis, Univ. of Innsbruck, 173 pp.
Ostermann, M., Sanders, D., Kramers, J., 2006. $^{230}Th/^{234}U$ ages of calcite cements of the proglacial valley fills of Gamperdona and Bürs (Riss ice age, Vorarlberg, Austria): geological implications. Austrian Journal of Earth Sciences 99, 31–41.
Ostermann, M., Sanders, D., Prager, C., Kramers, J., 2007. Aragonite and calcite cementation in 'boulder-controlled' meteoric environments on the Fern Pass rockslide (Austria): implications for radiometric age-dating of catastrophic mass movements. Facies 53, 189–208.
Patzelt, G., 1980. Neue Ergebnisse der Spät- und Postglazialforschung in Tirol. Jahresberichte der Österreichischen Geographischen Gesellschaft, 76/77, pp. 11–18.
Patzelt, G., 1987. Untersuchungen zur nacheiszeitlichen Schwemmkegel- und Talentwicklung in Tirol. Veröffentlichungen des Tiroler Landesmuseums Ferdinandeum 67, 93–123.
Patzelt, G., Resch, W., 1986. Quartärgeologie des mittleren Tiroler Inntales zwischen Innsbruck und Baumkirchen. Jahresberichte und Mitteilungen der oberrheinischen geologischen Vereinigung, Neue Folge 68, 43–66.
Piller, W.E., Egger, H., Erhart, C.W., et al., 2004. Die stratigraphische Tabelle von Österreich 2004 (sedimentäre Schichtfolgen). Gerin Druck, Wolkersdorf.
Prager, C., Zangerl, C., Patzelt, G., Brandner, R., 2008. Age distribution of fossil landslides in the Tyrol (Austria) and its surrounding areas. Natural Hazards and Earth System Science 8, 377–407.
Preusser, F., 2004. Towards a chronology of the Late Pleistocene in the northern Alpine foreland. Boreas 33, 195–210.
Reitner, J.M., 2007. Glacial dynamics at the beginning of Termination I in the Eastern Alps and their stratigraphic implications. Quaternary International 164–165, 64–84.
Sanders, D., 2008. Eislast-Erscheinungen und Intraklasten in der Höttinger Brekzie (Riß-Würm Interglazial) bei Innsbruck (Österreich). Geo. Alp 5, 149–164.
Sanders, D., 2010. Sedimentary facies and progradational style of a Pleistocene talus-slope succession, Northern Calcareous Alps, Austria. Sedimentary Geology 228, 271–283.
Sanders, D., Ostermann, M., Kramers, J., 2009. Quaternary carbonate-rocky talus slope successions (Eastern Alps, Austria): sedimentary facies and facies architecture. Facies 55, 345–373.
Sanders, D., Ostermann, M., Kramers, J., 2010. Meteoric diagenesis of Quaternary carbonate-rocky talus slope successions (Northern Calcareous Alps, Austria). Facies 56, 27–46.
Schlager, W., 2004. Fractal nature of stratigraphic sequences. Geology 32, 185–188.
Schmid, S.M., Fügenschuh, B., Kissling, E., Schuster, R., 2004. Tectonic map and overall architecture of the Alpine orogen. Eclogae Geologicae Helvetiae 97, 93–117.
Schrott, L., Hufschmidt, G., Hankammer, M., Hoffmann, T., Dikau, R., 2004. Spatial distribution of sediment storage types and quantification of valley fill deposits in an alpine basin, Reintal, Bavarian Alps, Germany. Geomorphology 55, 45–63.
Stingl, V., 1989. Marginal marine sedimentation in the basal Alpine Buntsandstein (Scythian) in the western part of the Northern Calcareous Alps (Tyrol/Salzburg, Austria). Palaeogeography, Palaeoclimatology, Palaeoecology 72, 249–262.
Thompson Davis, P., Menounos, B., Osborn, G., 2009. Holocene and latest Pleistocene alpine glacier fluctuations: a global perspective. Quaternary Science Reviews 28, 2021–2033.
Tinner, W., Theurillat, J.-P., 2003. Uppermost limit, extent, and fluctuations of the timberline and treeline ecoline in the Swiss Central Alps during the past 11,500 years. Arctic, Antarctic, and Alpine Research 35, 158–169.
Van Husen, D., 1977. Zur Fazies und Stratigraphie der jungpleistozänen Ablagerungen im Trauntal. Jahrbuch der Geologischen Bundesanstalt 120, 1–130.
Van Husen, D., 1983. General sediment development in relation to the climatic changes during Würm in the eastern Alps. In: Evenson, E.B., Schlüchter, Ch., Rabassa, J. (Eds.), Tills and Related Deposits. A. A. Balkema, Rotterdam, pp. 345–349.
Van Husen, D., 2000. Geological processes during the Quaternary. Mitteilungen der Österreichischen Geologischen Gesellschaft 92, 135–156.
Van Husen, D., 2004. Quaternary glaciations in Austria. In: Ehlers, J., Gibbard, P.L. (Eds.), Quaternary Glaciations-Extent and Chronology. : Developments in Quaternary Science, 2. Elsevier, Amsterdam, pp. 1–13.
Van Vliet-Lanoe, B., 1976. Traces de ségrégation de glace en lentilles associées aux sols et phénomènes périglaciaires fossiles. Biuletyn Periglacjalny 26, 41–55.
Van Wagoner, J.C., Posamentier, H.W., Mitchum, R.M., Vail, P.R., Sarg, R.F., Loutit, T.S., Hardenbol, J., 1988. An overview of the fundamentals of sequence stratigraphy and key definitions. In: Wilgus, C.K., Hastings, B.S., Ross, C.A., Posamentier, H.W., Kendall,, C.G.St.C. (Eds.), Sea-Level Changes — An Integrated Approach: Society of Economic Paleontologists and Mineralogists Special Publication, 42, pp. 39–45.
Wurth, G., Niggemann, S., Richter, D.K., Mangini, A., 2004. The Younger Dryas and Holocene climate record of a stalagmite from Hölloch Cave (Bavarian Alps, Germany). Journal of Quaternary Science 19, 291–298.